

# Surface functionalization of titanium with silver nanoparticles

A Sharonova<sup>1</sup>, M Surmeneva<sup>1</sup>, K Loza<sup>2</sup>, O Prymak<sup>2</sup>, M Epple<sup>2</sup> and R Surmenev<sup>1\*</sup>

<sup>1</sup>Research centre for physical materials science and composite materials, *National Research Tomsk Polytechnic University*, 30 Lenin Avenue, Tomsk 634050, Russian Federation

<sup>2</sup>Institute of Inorganic Chemistry, *University of Duisburg-Essen*, 7 University Street, Essen 45141, Germany

\*E-mail: rsurmenev@mail.ru

**Abstract.** This study aims to investigate the most efficient ways for metallic samples functionalization with silver nanoparticles (AgNPs). Three different techniques of surface functionalization have been used for the coating of titanium metal, i.e. the sessile drop method (evaporation), dip-coating and electrophoretic deposition (EPD). AgNPs stabilized with polyvinylpyrrolidone had a spherical shape and the metallic core diameter, charge and polydispersity index were  $70 \pm 20$  nm, -15 mV and 0.192, respectively. SEM analysis revealed that AgNPs were homogeneously distributed over the entire surface and did not form the particle agglomerates only in case of EPD. Thus, EPD method and spherical AgNPs can be used for further investigation concerning the preparation of biocomposites with antibacterial and bioactive properties.

## 1. Introduction

Nowadays, the number of implants placed in the jaws constantly increased promoting development of novel materials and techniques based on collective clinical experience. Metals have a long history in dental and orthopedic treatment. Wide use of pure titanium in dentistry and orthopedics is due to the fact that it has good biocompatibility and mechanical stability. The process of osteointegration plays a critical role in dental implantation and provides an opportunity to form a stable bond of the implant with bone tissue [1,2]. The result of implantation largely depends on the response of the surrounding tissues to a foreign material that can cause fibrosis, inflammation and giant cell formation [3]. Consequently, the task of biomedical materials scientists is the formation of biocompatible and antibacterial implant surfaces for medical purposes. It is also important to form a structural and functional connection between organized vital bone and the surface of a titanium implant, capable of bearing the functional load [4]. Furthermore, biomaterials should support cell attachment, migration, proliferation, and stimulate regeneration [5], which allow to avoid rejection and speed up the treatment and recovery process [6,7].

The coatings composed of noble metal nanoparticles (typically, Au or Ag) have currently attained a wide attention and increased research interest. The antibacterial properties of silver have a long history in all cultures around the world. Modern techniques used in biotechnology has enabled the incorporation of ionizable silver into fabrics for clinical use. Silver is used for medical purposes in dressings, antibacterial creams, surgical appliances, endotracheal tubes, cardiac devices, bone prostheses and other devices [8-10]. The antibacterial effect of silver or silver compounds is based on the release of bioactive silver ions ( $\text{Ag}^+$ ) and their interaction with fungal or bacterial cell membranes.



Silver in metallic form and inorganic silver compounds are ionized in the presence of tissue exudates or body fluids. The silver ions have a low toxicity, therefore, they are able to minimize the risk of rejection due to clinical use in the human body [11-13].

The recent methods available for the fabrication of antibacterial films include physical and chemical techniques such as vacuum evaporation [14], chemical vapor deposition [14], laser-assisted vacuum deposition [15], sol-gel method [16], electro-deposition [17], etc. Most of the presented techniques have a limited option of process control parameters; they need complicated expensive equipment, etc. Some simple approaches such as dip coating and electrochemical deposition, have shown a great convenience in large-scale fabrication and much less defectiveness that is the way these techniques can easily produce thin coatings on large areas [18,19].

The present paper considered a series of rapid and simple methods of silver coatings fabrication such as dip coating, sessile drop and electrophoretic deposition (EPD) at room temperature. This was done to determine the most efficient method, which can be used in further to prepare the biocomposites with antibacterial and bioactive properties.

## 2. Materials and methods

### 2.1. Synthesis of PVP-stabilized AgNPs

Negatively charged silver nanoparticles (AgNPs) were synthesized by a wet chemical reduction method according to the results of the studies [20-23]. The method based on the reduction of silver nitrate using glucose as a reductant and polyvinylpyrrolidone as a stabilizer. At the first stage, 2 g glucose and 1 g PVP were dissolved in 40 g distilled water and then were heated up to 90 °C. Then 0.5 g AgNO<sub>3</sub> dissolved in 1 mL of distilled water was quickly added. Finally, the dispersion was kept at 90 °C for 1 h and then left to cool at room temperature. The synthesis was carried out under continuous vigorous stirring while the system was heated in a silicon oil bath. PVP-stabilized AgNPs were collected by ultracentrifugation using ultracentrifuge (Thermo Scientific) Sorvall WX Ultra Series, redispersed in distilled water and collected again by ultracentrifugation (3 times, 66 150 g / 30 000 rpm, 30 min). Thereby NO<sub>3</sub><sup>-</sup> molecules, excess glucose and its oxidation products, PVP excess, and Ag<sup>+</sup> excess were all removed. After that the AgNPs were re-dispersed in distilled water by ultrasonication (Ultrasonic bath (Elma) Elmasonic S10). The silver concentration was determined by atomic adsorption spectroscopy (AAS) using atomic absorption spectrometer (Thermo Electron Corporation) M-Series. Silver nitrate (Fluker, p.a.), glucose (D-(+)-glucose, Baker) and polyvinylpyrrolidone (PVP K30 Povidon 30; Fluka, molecular weight 40000 g mol<sup>-1</sup>) were used.

### 2.2. Substrate preparation

The commercially pure titanium (99.58 wt% titanium; 0.1 wt% oxygen; 0.15 wt% iron; 0.05 wt% carbon; 0.04 wt% nitrogen; 0.08 wt% silicon, plates 10×10 mm) was used as a substrate. The titanium samples were chemically etched for 5 to 10 s in acid mixture containing HF (48%) and HNO<sub>3</sub> (66%) dissolved in the distilled water with the ratio 1:2:2.5 in volume. After acid etching, the samples were ultrasonically washed (ultrasonic bath (Eurosonic Micro) Euronda SPA) sequentially in ethanol and demonized water for 10 minutes at room temperature.

### 2.3. Characterization methods

The hydrodynamic diameter (HDD) of the AgNPs was measured by two methods: dynamic light scattering (DLS) using a Zetasizer Nano ZS (Malvern, USA) and nanoparticle tracking analysis (NTA) using a NanoSight LN 10 equipment (Malvern, USA). In addition, the zeta (ζ) potential of the AgNPs was determined by DLS. Scanning electron microscopy (SEM) using an ESEM Quanta 400 FEG instrument (FEI) was used to estimate the size and morphology of AgNPs. The structure of the AgNPs was determined by the grazing incidence X-ray diffraction (GIXRD) at the incident beam angle of 2° and 2θ in the range from 5 to 110° with a step size of 0.05° (Panalytical Empyrean (Malvern, USA) instrument with Cu Kα radiation, 1.54 Å; 40 kV and 40 mA). The patterns of titanium (#44-1294) and

silver (#4-0783) from ICDD database were used as references. Rietveld refinement with the program package TOPAS 4.2 from Panalytical Empyrean instrument was performed for the calculation of an average crystallite size and lattice parameters

### 3. Results and discussion

#### 3.1. AgNPs characterization

DLS analysis shows that PVP-stabilized AgNPs have a polydispersity index (PDI) of 0.192, average HDD of 110 nm and  $\zeta$ -potential of around -15 mV. A low value of PDI (below 0.3) indicates the presence of a monodisperse system without of large agglomerates. Figure 1 illustrates the data for PVP-stabilized AgNPs with the dispersion time 1 hour. Thus, SEM images have shown that PVP-stabilized AgNPs have a spherical shape with a diameter of  $70 \pm 20$  nm.

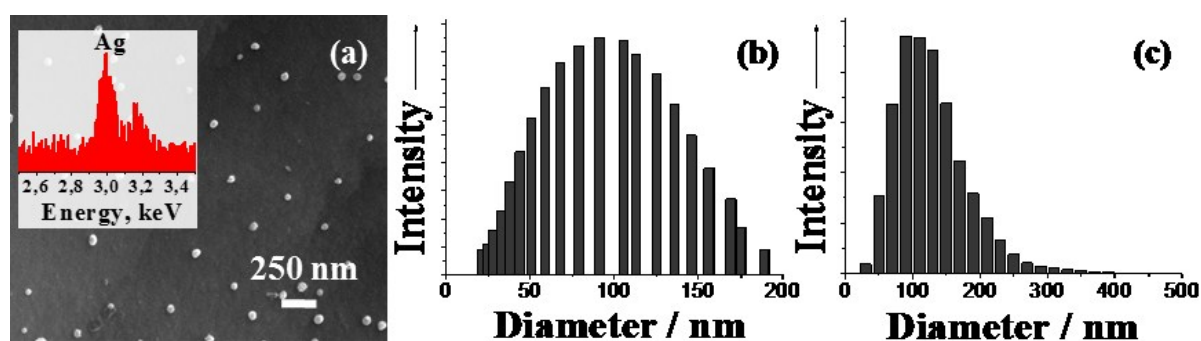


**Figure 1.** Silver nanoparticles. a) SEM image and EDX spectrum; b) DLS estimated distribution size of AgNPs, c) NTA estimated distribution size of AgNPs.

Particle size and shape play a key role in the antimicrobial activity. S. Banerjee et al. [24] demonstrated that nucleation occurs mainly at the beginning of the experiment and it is not continuous, although the particle size distribution becomes broader at a longer reaction time (10-120 nm, 30-3250 min). J. Helmlinger et al, [25] analyzed the biological effect of different AgNPs shapes on human mesenchymal stem cells. A toxic effect to human mesenchymal stem cells was observed at concentrations  $> 12.5 \text{ mg mL}^{-1}$ , but there was no significant influence of the particle shape on the cytotoxicity towards the cells. In addition to the biological effect of AgNPs, a particle shape-dependent effect on antibacterial activity was observed. AgNPs have shown the highest antibacterial effect ( $25 \text{ mg mL}^{-1}$ ), followed by spheres from glucose synthesis, spheres from the microwave synthesis, rods, and finally cubes. This toxic effect towards *S. aureus* correlates to the silver ion release. Nevertheless Loza et al. [21] reported that AgNPs (PVP-stabilized, 70 nm) affected the viability of *S. aureus* colonies. In that study antimicrobial activity of AgNPs was tested using standard methods that determine the minimum inhibitory and bactericidal concentration. *S. aureus* ( $10^6$  cells  $\text{mL}^{-1}$  in medium) was treated without (*S. aureus* in pure medium: positive control; pure medium: negative control) or with  $50 \text{ mg mL}^{-1}$  or  $30 \text{ mg mL}^{-1}$  of AgNPs for 24 h under cell culture conditions. Subsequently, the bacteria were plated and incubated for further 24 h at  $37^\circ\text{C}$  on blood agar plates. From the reported experiments and available literature on the dissolution of AgNPs, it was concluded that the particles could be dissolved after coming into contact with air, therefore they would become increasingly bactericidal (and cytotoxic) with time.

#### 3.2. Methods of titanium substrate functionalization with AgNP

The deposition of the PVP-stabilized AgNPs on titanium substrate was carried out via three different approaches. The first and easiest approach was drop casting or sessile drop. The process of sessile drop method is based on the formation of a droplet of  $120 \mu\text{L}$  in volume of a solution with the concentration  $60 \mu\text{g mL}^{-1}$  followed by drying at  $55^\circ\text{C}$ . The second method was dip-coating where the

sample was dipped in 5 mL of the solution with the same concentration and kept for 24 hours followed by drying at 55°C. One more method was EPD of PVP-stabilized AgNPs on titanium substrate. Prior to EPD, two types of working solutions were prepared. The first one was distilled water and the second was ethanol with the concentration of AgNPs 60  $\mu\text{g mL}^{-1}$ . The AgNPs were deposited on titanium substrates (10×10×2 mm) by immersion the substrate in the AgNPs suspension in a stainless steel cell (inner dimensions; diameter 18 mm and height 5 mm) and application of a voltage between the substrate and the EPD cell counter using a DC power supply. The distance between the substrate and the EPD cell was 2 mm in all experiments. The deposition time was 60 min and voltage 3 V in case of water solution. The deposition time was 30 min and voltage 50 V in case of ethanol solution. EPD was done via the motion of the charged PVP- stabilized AgNPs, dispersed in ethanol, towards an electrode under an applied electric field towards the metal surface of opposite charge. The electrophoretic motion of the charged particles during EPD results in the accumulation of particles and formation of a homogeneous and rigid deposit at the relevant (deposition) electrode-titanium sample [26]. Figure 2 shows the results of titanium substrate functionalization with AgNPs.

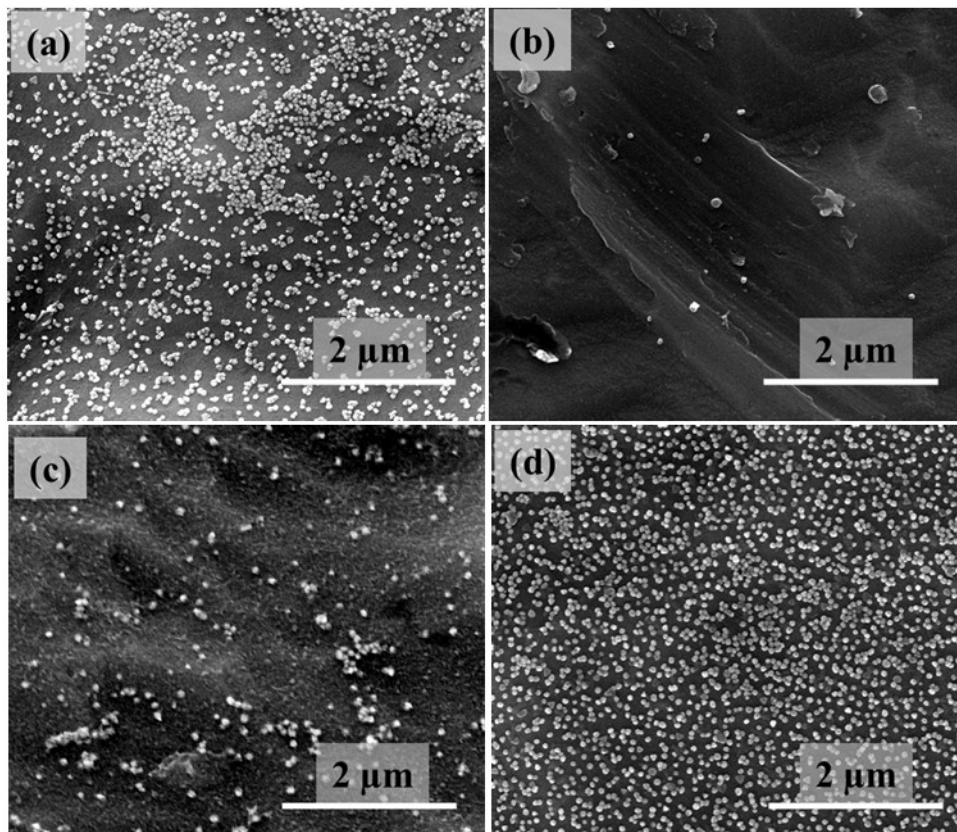


**Figure 2.** Titanium substrate functionalized with PVP-stabilized AgNPs (white spots) a) sessile drop 120  $\mu\text{L}$ , b) dip-coating, c) EPD in water (3 V, 60 min), d) EPD in ethanol (50 V, 30 min). The concentration of the solution was 60  $\mu\text{g mL}^{-1}$  in each experiment.

Figure 2 shows that the most effective methods for surface functionalization are sessile drop and EPD. SEM analysis confirmed the ability to attain a uniform distribution of the AgNPs layer in case of EPD method. However, sessile drop method has the disadvantage connected with the surface tension and therefore, the samples can not be fully coated with the particles. Thus, the sessile drop method has the disadvantage associated with the homogeneous deposition on specifically designed implants. The amount of silver was calculated using AAS data (table 1). These results have shown that EPD and

sessile drop methods provided the highest content of silver 14 and 7  $\mu\text{g}/\text{cm}^2$ , respectively. Thus, this method can be used to cover the implants of a complex shape.

**Table 1.** The amount of Ag per  $\text{cm}^2$  in dependence with the deposition method.

Method	Amount of Ag, $\mu\text{g}/\text{cm}^2$
Dip-coating	<1
EPD in water (3 V, 60 min)	5 $\pm$ 3
EPD in ethanol (50 V, 30 min)	14 $\pm$ 3
Sessile drop	7 $\pm$ 2

### 3.3. Structural investigation of AgNPs layer

Figure 3 shows the results of GIXRD obtained for the substrates functionalized with AgNPs by EPD and sessile drop methods. Table 2 presents the obtained results using Rietveld analysis.

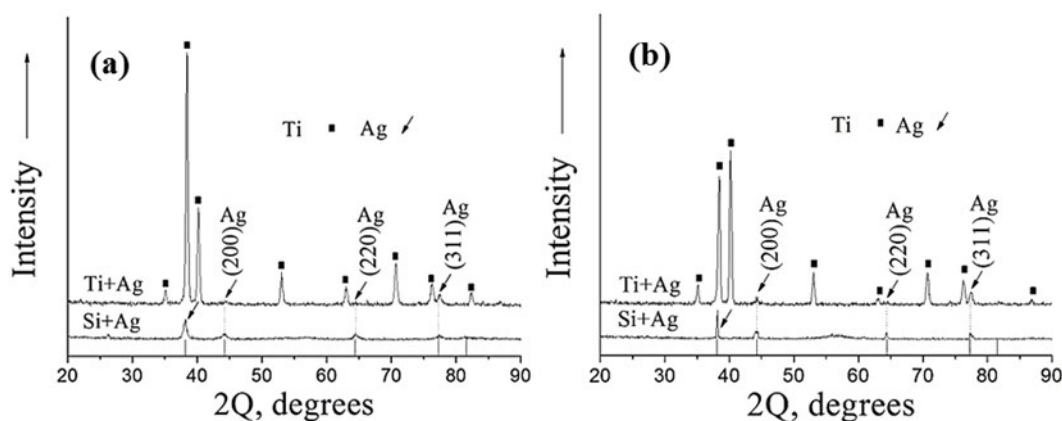


**Figure 3.** GIXRD patterns of the AgNPs layer on titanium and silicon substrates prepared by a) sessile drop, and b) EPD, where deposition time is 30 min, solution concentration 60  $\mu\text{g mL}^{-1}$ .

GIXRD patterns of titanium substrate functionalized via sessile drop method and EPD have shown the presence of reflexes at 2 Theta angles of 44.3° and 77.3°, which correspond to (200) and (311) planes of pure silver. Since the main reflections of titanium and silver phases were very close, we used a silicon substrate to control the silver content.

**Table 2.** Parameters calculated for AgNPs on titanium and silicon substrates. Ag  $a = 4.086 \text{ \AA}$  (ICDD)\*.

Sample	GSR, nm	Lattice parameters		
		$a=b, \text{ \AA}$	$c, \text{ \AA}$	$V, \text{ \AA}^3$
Ti substrate	Ti	110	2.950	35.315
	Ag	13	4.085	68.22
Si substrate	Ag	14	4.093	68.52

\*The data from ICDD database

A typical GIXRD pattern, obtained for silicon substrate used for the control of silver, illustrates the formation of intense lines for silver reflection (figure 3). The presence of the peaks are detected at 2  $\theta$

values  $38.1^\circ$ ,  $44.3^\circ$ ,  $64.4^\circ$  and  $77.3^\circ$  corresponded to (111), (200), (220), and (311) planes of silver, respectively. Thus, GIXRD pattern confirmed the cubic crystalline structure of silver. The crystallite size of the AgNPs was calculated by Rietveld analysis based on the obtained GIXRD results. The average crystallite sizes of AgNPs estimated from GIXRD patterns were 13 and 14 nm on silicon and titanium substrate, respectively (Table 2). The determined unit cell parameters were  $a=4.085 \text{ \AA}$  and  $a=4.093 \text{ \AA}$  in the case of titanium and silicon substrate, respectively (Table 2). The determined unit cell parameters were in good agreement with that of silver standard (ICDD, #4-0783,  $a=4.086 \text{ \AA}$ ) proved also in [24, 25].

#### 4. Conclusion

Functionalization of titanium substrate surface with AgNPs was carried out via sessile drop, dip-coating and EPD methods. According to the SEM data, EPD was the most efficient approach for surface functionalization. The PVP-stabilized AgNPs were synthesized in aqueous solution with a diameter of  $70 \pm 20 \text{ nm}$ , negative charge of  $-15 \text{ mV}$  and PDI of 0.192. The GIXRD data obtained for the PVP-stabilized AgNPs on titanium substrate have revealed typical peaks of silver at  $2\theta$  of  $44.3^\circ$  and  $77.3^\circ$  with the coherent scattering region of 14 nm. Thus, EPD approach will be used in our further research for functionalization of the HA coatings and fabrication of antibacterial biocomposites for biomedical application.

#### 5. Acknowledgments

We would like to thank the Euro-Russian Academic network for generous support in the framework of the Eranet Mundes Program. This research was supported by the Russian President's Stipend SP-444.2016.4. We thank the Deutsche Akademische Austauschdienst (DAAD) for funding within the Leonhard-Euler program. The research was carried out at Tomsk Polytechnic University within the framework of Tomsk Polytechnic University Competitiveness Enhancement Program grant and state order NAUKA (11.7293.2017/8.9; 11.1233.2017/4.6) and Russian President fellowship for young candidate of sciences (MK-6287.2018.8).

#### References

- [1] Hanawa, T 2010 Biofunctionalization of titanium for dental implant *Jpn. Dent. Sci. Rev.* **46/2** 93
- [2] Guo C Y, Matinlinna J P, and Hong Tang A T 2012 Effects of surface charges on dental implants: past, present, and future *Int. J. Biomater.* **2012** 381535
- [3] International Agency for Research on Cancer 1999 *Surgical Implants and Other Foreign Bodies* (Lyon: IARC Press) p 423
- [4] Johansson K, Jimbo R, Östlund P, Tranæus S and Becktor JP 2017 Effects of bacterial contamination on dental implants during surgery: a systematic review *Implant Dent.* **26/5** 778
- [5] Francis R, Kumar D S 2016 *Biomedical Applications of Polymeric Materials and Composites* (John Wiley & Sons) p 416
- [6] Lilja M 2013 *Bioactive Surgical Implant Coatings with Optional Antibacterial Function* (Uppsala: Acta Universitatis Upsaliensis) p 62
- [7] Khalid M D, Zafar M S, Farooq I, Khan R S and Najmi A 2017 Bioactive Glasses and their Applications in Dentistry *JPDA* **26/01** 33
- [8] Zhu S Q, Zhang T, Guo X L, Wang Q L, Liu X F and Zhang X Y 2012 Gold nanoparticle thin films fabricated by electrophoretic deposition method for highly sensitive SERS application *Nanoscale Res. Lett.* **7/1** 613
- [9] Baino F, Perero S, Miola M, Ferraris M 2017 Antibacterial Nanocoatings for Ocular Applications *Adv. Sci. Technol.* **102** 24
- [10] Spagnol C, Fragal E H, Pereira A G, Nakamura C V, Muniz E C, Follmann H D, Silva R, Rubira A F 2018 Cellulose nanowhiskers decorated with silver nanoparticles as an additive

- to antibacterial polymers membranes fabricated by electrospinning *J. Colloid Interf. Sci.* **531** 705
- [11] Martins da Silva L H, Rai M, Neto J M and Gomes P W P 2018 *Silver: Biomedical Applications and Adverse Effects Biomedical Applications of Metals* (Springer International Publishing AG, part of Springer Nature) p 113
- [12] Hoa V X 2018 Study of synthesis silver nanoparticles for antibacterial activity against of Escherichia coli and Staphylococcus aureus application *Adv. Nat. Sci. Nanosci.* **9/2** 2043
- [13] Balakrishnan S, Sivaji I, Kandasamy S, Duraisamy S, Kumar N S and Gurusubramanian G 2017 Biosynthesis of silver nanoparticles using Myristica fragrans seed (nutmeg) extract and its antibacterial activity against multidrug-resistant (MDR) Salmonella enterica serovar Typhi isolates *Env. Sci. Pollut. R.* **24/17** 14758
- [14] Sunandana C S 2015 *Introduction to Solid State Ionics: Phenomenology and Applications* (CRC Press.) p 529
- [15] Morintale E, Constantinescu C and Dinescu M 2010 Thin films development by pulsed laser-assisted deposition *Physics AUC* **20/1** 43
- [16] Raheem Ka G and Seror Hameed H 2015 CdO: Ag films deposited by sol-gel process: a study on their structure and optical properties *IJSR* **4/6** 1361
- [17] Eom H, Jeon B, Kim D and Yoo B 2010 Electrodeposition of silver-nickel thin films with a galvanostatic method *Mater. Trans.* **51/10** 1842
- [18] Rajabi N, Heshmatpour F, Malekfar R, Bahari-Poor H R and Abyar S 2014 A comparative study of dip coating and spray pyrolysis methods for synthesizing ITO nanolayers by using Ag colloidal sol *Mater. Sci. Poland* **32/1** 102
- [19] Wei L, Lu J, Xu H, Patel A, Chen Z S and Chen G 2015 Silver nanoparticles: synthesis, properties, and therapeutic applications *Drug Discovery Today* **20/5** 595
- [20] Wang H, Qiao X, Chen J, Ding S 2005 Preparation of silver nanoparticles by chemical reduction method *Colloids and Surfaces A: Physicochemical and Engineering Aspects* **256/2-3** 111
- [21] Loza K, Diendorf J, Sengstock C, Ruiz-Gonzalez L, Gonzalez-Calbet J M, Vallet-Regi M, Köller M and Epple M 2014 The dissolution and biological effects of silver nanoparticles in biological media *J. Mater. Chem. B* **2/12** 1634
- [22] Sahoo P K, Kamal S K, Kumar T J, Sreedhar B, Singh A K and Srivastava S K 2009 Synthesis of silver nanoparticles using facile wet chemical route *Defence Sci. J.* **59/4** 447
- [23] Sharonova A, Loza K, Surmeneva M, Surmenev R, Prymak O and Epple M 2016 Synthesis of positively and negatively charged silver nanoparticles and their deposition on the surface of titanium *IOP Conf. Ser. Mater. Sci. En.* **116/1** 012009
- [24] Banerjee S, Loza K, Meyer-Zaika W, Prymak O, Epple M 2014 Structural evolution of silver nanoparticles during wet-chemical synthesis *Chem. Mater.* **26/2** 951
- [25] Helmlinger J, Sengstock C, Groß-Heitfeld C, Mayer C, Schildhauer T A, Köller M and Epple M 2016 Silver nanoparticles with different size and shape: equal cytotoxicity, but different antibacterial effects *RSC Advances* **6/22** 18490
- [26] Besra L and Liu M 2007 A review on fundamentals and applications of electrophoretic deposition (EPD) *Prog. Mater. Sci.* **52/1** 1
- [27] Ivanova A A, Surmeneva M A, Tyurin A I, Pirozhkova T S, Shuvarin I A, Prymak O, Epple M, Chaikina M V and Surmenev R A 2016 Fabrication and physico-mechanical properties of thin magnetron sputter deposited silver-containing hydroxyapatite films *Appl. Surf. Sci.* **360** 929
- [28] Ivanova A A, Surmenev R A, Surmeneva M A, Mukhametkaliyev T M, Sharonova A A, Grubova I Y, Loza K, Chernousova S, Prymak O and Epple M 2014 Antibacterial AgNPs/CaP biocomposites *Strategic Technology (IFOST)* **2014** 472